Program DYNAFIT for the Analysis of Enzyme Kinetic Data: Application to HIV Proteinase

Petr Kuzmič

School of Pharmacy and Department of Chemistry, University of Wisconsin, 1101 University Avenue, Madison, Wisconsin 53706; and BioKin, Ltd., 1601 Adams Street, Madison, Wisconsin 53711

A computer program with the code name DYNAFIT was developed for fitting either the initial velocities or the time course of enzyme reactions to an arbitrary molecular mechanism represented symbolically by a set of chemical equations. Seven numerical tests and five graphical tests are applied to judge the goodness of fit. Experimental data on the inhibition of the dissociative dimeric proteinase from HIV were used in four test examples. A set of initial velocities was analyzed to see if a tight-binding inhibitor could bind to the HIV proteinase monomer. Three different sets of progress curves were analyzed (i) to determine the kinetic properties of an irreversible inhibitor, (ii) to investigate the dissociation and denaturation mechanism for the protease dimer, and (iii) to investigate the inhibition mechanism for a transient inhibitor. The program is available by anonymous ftp via uwmml.pharmacy.wisc.edu and on the World Wide Web via http://uwmml.pharmacy.wisc.edu. © 1996 Academic Press, Inc.

This paper describes a novel computational tool for mechanistic enzyme kinetics, the program DYNAFIT. Given a set of initial reaction velocities, or a set of progress curves from enzyme reactions, the program fits the data to an arbitrary reaction mechanism represented symbolically by a set of chemical equations. There are no other methods that can be used to fit initial velocities to a set of chemical equations. Certain well-known programs (1, 2) use chemical equations as input for simulations of progress curves, but DYNAFIT surpasses them in four important respects. First, DYNAFIT can handle progress curves from concentration jump experiments, as is explained below. Second, DYNAFIT can simulate and fit progress curves with the involvement of preexisting isomerization equilibria. Third, DYNAFIT considers concentrations as unknown if necessary. This capability is required to achieve a satis-factory fit of more than one progress curve to the same set of rate constants, and it can be used for active-site titrations. Finally, DYNAFIT can treat as adjustable parameters certain instrumental parameters, such as baseline signal or molar absorptivity.

Classical enzyme kinetics (3–5) is concerned with fitting a set experimental data to a single algebraic equation, namely the exact or analytical rate equation based on the postulated reaction mechanism. The goal is to determine the value of certain kinetic constants or, more importantly, to see if the mechanism fits the data. For many important mechanisms, such as tight-binding inhibition of dissociative dimeric enzymes (retroviral proteinases, integrases, and reverse transcriptases), the exact rate equation unfortunately cannot be derived. In order to determine the inhibition constants or validate a postulated inhibition mechanism, one must resort to an inexact or finite-difference solution of a complete system of algebraic and differential equations.

The exact rate equations of classical enzyme kinetics, such as the Michaelis–Menten equation, can be evaluated with little computational effort. Given the concentration of the substrate and the enzyme and given the values of k_{cat} and K_M, one can compute the steady-state velocity by hand, because only a few arithmetic operations (additions, multiplications, and divisions) are involved. In contrast, the approximate, iterative solution of the complete systems of differential equations usually includes millions of arithmetic operations and thus can be performed only by a machine.

This new computational enzyme kinetics was presaged by Garfinkel *et al.* (6) and pioneered by computer programs KINSIM (1) and FITSIM (2). The new numerical approach was systematized in an introductory monograph (7). The starting point for our research was the realization that the existing computer programs have fundamental defects. They cannot simulate or fit initial reaction velocities, cannot analyze concentration

jump experiments, do not take into account titration errors, and do not allow for uncertainties in instrumental parameters such as baseline absorbance or molar absorption coefficients. Program DYNAFIT described in this paper remedies these deficiencies.

METHODS

This section presents an outline of the most important theoretical principles used in DYNAFIT. Several established computational methods mentioned below were modified to suit the analysis of enzyme systems, and other algorithms were developed *de novo.* No attempt is made at a rigorous description of technical details, which will be given in a specialized account elsewhere.

Computation of multiple simultaneous equilibria. To compute the composition at equilibrium of an arbitrary mixture of biochemical reactants, DYNAFIT uses a stripped-down version of the program EQUIL (8), based on the multidimensional Newton–Raphson method. The original algorithm was simplified by eliminating most devices that enforce convergence [for details see (8)]. Only a simple check was retained to prevent the occurrence of negative concentrations as intermediate results.

Computation of reaction progress curves. A modification of the Livermore solver of ordinary differential equations [LSODE (9)] was employed to compute progress curves. The backward differentiation formula with full analytical Jacobian is used, along with stringent error tolerances (absolute error 10^{-20} M, relative error 10^{-8}). Changes in LSODE, inspired by the design of the differential-algebraic solver DASSL (10), were introduced to prevent negative concentrations from arising during the computation.

Least-squares regression. A variation of the Levenberg–Marquardt algorithm due to Reich (11) was further modified, to allow optional restarts whenever the weighted sum of squared deviations increases. Restarts are attempted also when the algorithm reaches a minimum on the least-squares hypersurface (12). In some cases these restarts guide the Levenberg–Marquardt–Reich minimization out of a shallow false minimum. The following physical quantities can be treated as adjustable parameters: (i) rate constants, (ii) analytic concentrations of reactants, (iii) molar response coefficients (e.g., the molar absorbance coefficients in spectrophotometry), and (iv) the instrumental offset (e.g., absorbance at Time 0). Some authors have used a rational power function (13) to describe the experimental variances; we use instead a cubic polynomial.
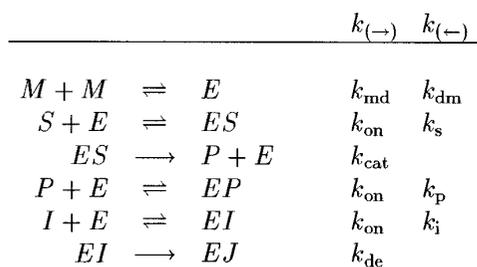
Numerical tests of goodness of fit. Seven numerical tests are used to diagnose the goodness of fit to a given model. (i) The incomplete gamma function (14) mea-sures the probability that the reduced χ^2 (15) could arise by pure chance. (ii) The average deviation measures the systematic bias of the fit. (iii) The randomness in the runs of the same signs of residuals (16) is expressed as a probability that any given run of signs is entirely random (e.g., $+++---+--+--+++++$ $----+$ has probability of randomness 3.5%). (iv) The continuous criterion for the goodness of fit (17) is a pass–fail test, at the 5% confidence level, that the residuals of fit come from the normal distribution. (v) The Kolmogorov–Smirnov statistic (14) also measures the probability that the residuals follow the normal or Gaussian distribution. (vi) The Durbin–Watson statistic (12, 18) measures the probability that the residuals of fit might be serially correlated, which indicates a lack of fit. (vii) The Tukey statistics $T_{1,1}$ and $T_{1,2}$ (18) diagnose various types of systematic misfit.

Graphical tests of goodness of fit. Five graphical techniques are used to diagnose lack of fit, manifested by nonrandom patterns in the residuals. (i) For a successful fit, the residuals plotted against the independent variable (e.g., time or concentration) should be symmetrically distributed about the horizontal axis (19). (ii) Even more expressive are plots of residuals against the dependent variable (e.g., absorbance or velocity) (16, 18). (iii) The histogram of standardized residuals should have the characteristic bell shape. (iv) The normal plot of standardized ordered residuals (20) should be linear for a good fit, and the slope of this plot, i.e., the standard deviation, should be close to unity. (v) The empirical cumulative distribution function (20) should follow the cumulative normal distribution (21).

Redundancy of fitting parameters. Five numerical criteria are used to assess the uncertainties of fitting parameters, their mutual dependence, and redundancy in the given model. (i) The formal standard errors of fitting parameters, defined as the square roots of the diagonal elements of the variance–covariance matrix (14), are a crude approximation to true uncertainties. (ii) The asymptotic correlation matrix (16) and (iii) the variance inflation factors (16) measure the overall codependency of fitting parameters. (iv) The condition numbers, defined as the ratios of eigenvalues of the scaled information matrix over the smallest eigenvalue (22), reveal the presence of a possibly redundant combination of fitting parameters. (v) The corresponding eigenvectors (22) describe such redundant combinations in detail.

Matrix formulation of reaction mechanisms. The symbolism of chemical equations is translated into the underlying systems of mathematical equations by using the theory of matrices (23). Formula matrices for the multiple equilibrium problem (24) are derived automatically, by using a modification of known matrix methods (25, 26). Linear algebraic methods are used

$$\begin{array}{lll} & & k_{(\rightarrow)} \quad k_{(\leftarrow)} \\ \hline M + M & \rightleftharpoons & E & k_{md} \quad k_{dm} \\ S + E & \rightleftharpoons & ES & k_{on} \quad k_{s} \\ ES & \longrightarrow & P + E & k_{cat} \\ P + E & \rightleftharpoons & EP & k_{on} \quad k_{p} \\ I + E & \rightleftharpoons & EI & k_{on} \quad k_{i} \\ EI & \longrightarrow & EJ & k_{de} \end{array}$$

SCHEME 1

also to transform equilibrium constants into the stability constants of molecular complexes (27), which are required for the computation of multiple simultaneous equilibria.

RESULTS

Typical results obtained by using program DYNAFIT are illustrated in this section by way of four examples taken from the inhibition kinetics of HIV proteinase. Each example represents one feature of the program which is absent in other known tools for the analysis of enzyme kinetic data: (i) the inclusion of titration errors, (ii) the concentration jump experiments, (iii) the preexisting isomerization equilibria, and (iv) the analysis of initial velocities. In some cases the structure of the HIV proteinase inhibitors was not known to this data analyst. The sample experimental data were provided for consultations by researchers in the academia and in the industry, as is gratefully acknowledged below. The structure of the inhibitors is not important here, because the sole purpose of this paper is to illustrate the basic functionality of a new program for kinetic analysis.

Example 1: Titration Errors

This example illustrates the importance of allowing for titration errors in the analysis of enzymatic progress curves. The HIV proteinase (assay concentration 0.004 μM) was added to a solution of an irreversible inhibitor and a fluorogenic substrate [25 μM (28)]. Five assays were conducted, at four different concentrations of the inhibitor (0, 0.0015, 0.003, and 0.004 μM in replicate). The fluorescence changes were monitored for 1 h in each experiment. The combined experimental data were fitted as a whole [global analysis (29)] to the reaction mechanism shown in Scheme 1. The results of the least-squares fit are summarized in Table 1 and in Fig. 1.

Figure 1 shows that program DYNAFIT was able to match the experimental data and the theoretical model in Scheme 1 reasonably well. The best-fit values of adjustable parameters in Table 1 mean that the irrevers-

ible inhibitor has an initial binding constant of 0.83 $\pm$ 0.02 nM and a deactivation rate constant of 0.122 $\pm$ 0.002 s^{-1}. In contrast, the program FITSIM (2) failed to match the data and the model and gave very different inhibition constants (0.0001 nM, 50 s^{-1}). A detailed comparison of the two programs is given in Discussion.

Note that the bimolecular association rate constants were set to the same value (10^8 M^{-1} s^{-1}) for the inhibitor, the substrate, and the product. In reality it is extremely unlikely that all three ligands would have exactly identical association rate constants. In this example we used a feasible identical value merely because the exact values cannot be determined from the sample data.

Example 2: Concentration Jump Experiments

This example illustrates the combination of computing multiple simultaneous biochemical equilibria (solving systems of algebraic equations) and computing the time course of biochemical reactions (solving systems of differential equations). This combination of different computing tasks is necessary to analyze progress curves obtained in the concentration jump experiments.

The purpose of the following two assays was to determine the dissociative properties of the HIV proteinase under the given set of experimental conditions, namely under vigorous mechanical stirring. In the first experiment (curve A in Fig. 2) the enzyme was kept in the stock solution at 1.5 μM. To initiate the reaction, a small aliquot of the enzyme solution was added to the rapidly stirred fluorogenic substrate, so that the final concentration was much lower in the assay (0.005 μM) than in the enzyme stock. The result of this dilution is that the enzyme dimer partially dissociates over time. In the second experiment (curve B in Fig. 2) the order of additions was reversed. The enzyme (0.005 μM) was first equilibrated in the rapidly stirred assay buffer, and the reaction was started by the addition of a very small volume of the substrate stock. An inverse process takes place, as the substrate induces assembly of the active dimer from inactive subunits (30). The two progress curves taken together were fitted to the kinetic model shown in Scheme 2. Figure 2 shows a very good match between the theoretical model and the experimental data. The numerical results are summarized in Table 2. Unlike Schemes 1 and 3, Scheme 2 does not include product inhibition, because in this particular example the corresponding rate constant k_p is not uniquely determined from the sample data and appears redundant in the fitting model.

The best-fit values of rate constants for association and dissociation of the monomer subunits (0.61 μM^{-1} s^{-1} and 0.0085 s^{-1}) give an equilibrium constant K_d 14 nM. These results are comparable with the published

TABLE 1

Results of the Least-Squares Fit of Progress Curves Shown in Figs. 1 (DYNAFIT) and 7 (FITSIM)
to the Kinetic Model Shown in Scheme 1

Dataset (trace)	Parameter	Initial value	Fitted value	
			DYNAFIT	FITSIM
	k_{md} (μM^{-1} s^{-1})	0.1	—	—
	k_{dm} (s^{-1})	0.001	—	—
	k_{on} (μM^{-1} s^{-1})	100	—	—
	k_s (s^{-1})	300	179.7 ± 2.0	118.4 ± 2.5
	k_{cat} (s^{-1})	10	9.46 ± 0.17	8.107 ± 0.093
	k_p (s^{-1})	500	1117 ± 16	668 ± 41
	k_i (s^{-1})	0.1	0.0831 ± 0.0018	0.000013 ± 0.03732
	k_{de} (s^{-1})	0.1	0.1224 ± 0.0022	50 ± 63512
	ϵ_P	0.024	0.0230 ± 0.0004	—
A	$[S]_0$ (μM)		25.72 ± 0.48	—
B			28.53 ± 0.50	—
C		25	24.63 ± 0.45	—
D			19.50 ± 0.71[a]	—
E			16.67 ± 0.75[a]	—
A	$[E]_0$ (μM)		0.00346 ± 0.00008	—
B			0.00492 ± 0.00004	—
C		0.004	0.00387 ± 0.00005	—
D			0.00418 ± 0.00004	—
E			0.00400 ± 0.00009	—
A	Offset		−0.006 ± 0.001	—
B			−0.023 ± 0.001	—
C		0	−0.010 ± 0.001	—
D			−0.019 ± 0.001	—
E			−0.008 ± 0.001	—

Note. The concentrations of the inhibitor were 0, 1.5, 3, 4, and 4 nM for traces A–E, respectively.

[a] The substrate concentrations are not well defined by progress curves collected at high inhibitor concentrations. The formal standard error does not reflect the true uncertainty in this case. The 68% confidence interval extends to approximately 25 μM.

rate constants (0.92 μM^{-1} s^{-1} and 0.0019 s^{-1}, K_d 4 nM) observed under different physical conditions (31), albeit in a similar experiment, where two progress curves with and without preincubation of the enzyme were combined for analysis. This combination of two otherwise identical progress curves, one with preincubation and one without it, has been shown theoretically (32) as the most effective experimental design for measuring the association and dissociation rate constants.

When the reaction step $ES \rightleftharpoons FS$ was omitted from the mechanism in Scheme 2, the data and the simplified fitting model did not match. The step represents a nonproductive isomerization of the ternary Michaelis complex, possibly due to subunit exchange. Remarkably, when the rapid mechanical stirring was turned off, the progress fit the simpler kinetic mechanism without nonproductive isomerization (data not shown). These results do not mean that the mechanism in Scheme 2 is necessarily correct. The anomaly in HIV proteinase kinetics, a denaturation introduced by mechanical stirring, might be explained by another unknown molecular mechanism. It is not our aim to investigate that mechanism. The sole purpose of Example 2

is to illustrate the capability of DYNAFIT to handle concentration jump experiments.

Example 3: Preexisting Isomerization Equilibria

This example is a variation on the concentration jump experiment described above. Here the unknown composition at the beginning of the assay is determined by isomerization equilibria, instead of association/dissociation equilibria. The problem arises typically in fitting transient inhibition data (Fig. 3) to a model which includes rapid interconversion between two or more different molecular forms of the inhibitor, such as rotational isomers, or different protonation states (Scheme 3).

The best-fit model parameters (Table 3) suggest that the transient phase in the inhibition kinetics could be caused by a minor molecular form of the inhibitor (e.g., a minor conformer) binding to the enzyme, while the rest of the inhibitor (96%) binds much less strongly. Even though the interconversion between the active and the inactive molecular forms of the inhibitor is virtually infinitely rapid, as would be the case for freely interconverting conformers, a transient phase is detect-
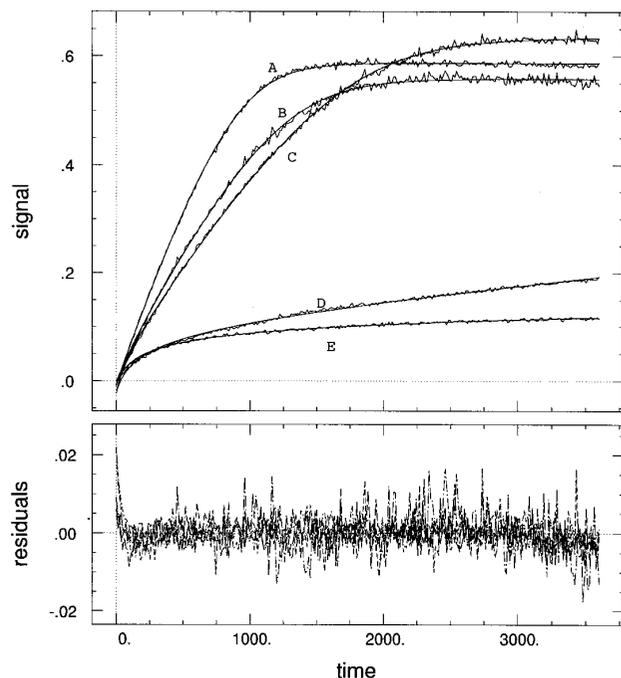
FIG. 1.   Global least-squares fit of progress curves collected during irreversible inhibition of the proteinase from HIV (nominal concentration 0.004 μM). The enzyme was the last added component in the assay. Inhibitor concentrations were held fixed at their nominal values: 0 μM (A), 0.0015 μM (B), 0.003 μM (C), and 0.004 μM (D and E). The nominal concentrations of the substrate (25 μM) and enzyme (0.004 μM) in each assay were optimized within $\pm$10% titration error. Fluorescence at Time 0 was also optimized for each assay. For comparison with FITSIM (see Fig. 5), the initial fluorescence signals were set to zero (baseline subtraction). For details see text; the numerical results are summarized in Table 1.
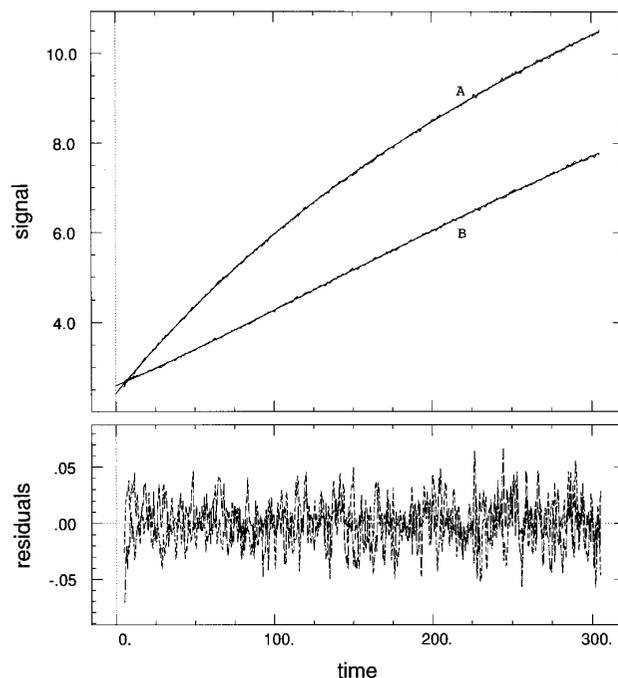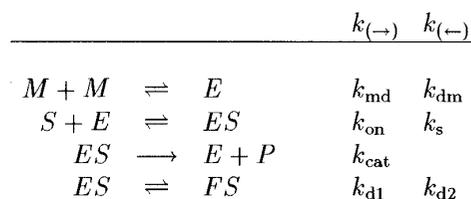
FIG. 2.   Global least-squares fit of progress curves collected during fluorescence assays of HIV proteinase [the paired progress curve method (32)]. Curve A, a 5-μl aliquot of the concentrated proteinse (stock 1.5 μM) was added into 1.495 ml of substrate solution (10 μM) in the rapidly stirred assay buffer. Curve B, the diluted proteinase (5 nM) was equilibrated for 15 min in 1.485 ml of the assay buffer under rapid stirring, and the reaction was started by the addition of the substrate (15 μl, stock 1.0 mM). Throughout the assay, the reacting mixture was continuously stirred in the cuvette compartment. For details see text; the numerical results are summarized in Table 2.

able nevertheless. The reason is that the population of the actively binding form is so small that diffusion control plays a role. It is possible that other mechanisms could explain the experimental data. The purpose of this paper is not to decide which is the most plausible mechanism. The only goal is to demonstrate that the computer program DYNAFIT, unlike other similar tools, can handle kinetic mechanisms that include pre-existing equilibria with unknown isomerization rate constants.

Example 4: Analysis of Initial Velocities

This example illustrates the fitting of initial velocities from enzyme assays to a molecular mechanism for which a classical rate equation cannot be derived. The question was whether observed dose–response curves for a tight-binding inhibitor (Fig. 4) could be consistent with binding to the inactive, monomeric form of the partially dissociated enzyme (Scheme 4). This simultaneous binding to the inactive monomer and to the active dimer would be a special case of the "mixed-type"

noncompetitive, tight-binding inhibition. The initial velocities were measured by using a method described elsewhere (33).

The numerical results of fitting the data in Fig. 4 to the model in Scheme 4 are summarized in Table 4. Binding of the inhibitor to the enzyme monomer probably does not occur, because the fitted value of the corresponding dissociation constant $MI \rightarrow M + I$ is very much larger than the dissociation constant for the EI complex. Similar results were obtained when the fitting model included the binding of the inhibitor to the Michaelis complex ES. The conclusion is that the tight-

			$k_{(\rightarrow)}$	$k_{(\leftarrow)}$
$M + M$	$\rightleftharpoons$	E	k_{md}	k_{dm}
$S + E$	$\rightleftharpoons$	ES	k_{on}	k_{s}
ES	$\longrightarrow$	$E + P$	k_{cat}	
ES	$\rightleftharpoons$	FS	k_{d1}	k_{d2}

SCHEME 2

TABLE 2

Results of the Least-Squares Fit of Progress Curves Shown in Fig. 2 to the Kinetic Model Shown in Scheme 2

Dataset (trace)	Parameter	Initial value	Fitted value
	k_{md} ($\mu M^{-1} s^{-1}$)	0.2	0.609 ± 0.014
	k_{dm} (s^{-1})	0.002	0.0085 ± 0.0004
	k_{on} ($\mu M^{-1} s^{-1}$)	100	—
	k_s (s^{-1})	300	250 ± 72
	k_{cat} (s^{-1})	10	10.29 ± 0.21
	k_{d1} (s^{-1})	0.004	0.00367 ± 0.00012
	k_{d2} (s^{-1})	0.002	0.00166 ± 0.00008
	ϵ_P	1.93	—
	$[S]_0$ (μM)	30	—
A	$[E]_0 + 2[M]_0$ (μM)	1.5^a	—
B		0.005^b	—
A	Offset	$—^c$	2.418 ± 0.004
B		$—^c$	2.591 ± 0.005

[a] Enzyme was added last. The distribution between the monomeric and the dimeric forms of the enzyme at the beginning of the assay was computed automatically from the total enzyme concentration in the stock ($[E]_0 + 2[M]_0$) and the dissociation constant $K_d = k_{dm}/k_{md}$. The initial concentration of M and E in the assay was computed from the concentration in the stock divided by the dilution ration (1:300).

[b] Substrate was added last. The dilution by substrate stock was neglected, so that the dilution ratio was taken as 1:1.

[c] The initial estimate of the offset was made automatically, by using the first datapoint on each progress curve.

binding inhibitor is strictly competitive with the substrate and does not interact with the enzyme monomer.

DISCUSSION

The most widely used programs for computational enzyme kinetics are KINSIM (1) for simulations and FITSIM (2) for least-squares fitting. FITSIM, which utilizes KINSIM to simulate progress curves during nonlinear least-squares regression, has been used in about a dozen laboratories to study the dihydrofolate reductase (34), adenosine deaminase (35), HIV protease (36) and reverse transcriptase (37), bacterial (38) and firefly luciferase (39), alcohol dehydrogenase (40), thrombin (41), phtalate dioxygenase reductase (42), DNA helicase (43), and gyrase (44). Other regression programs based on numerical integration of differential equations have been described recently, such as DNRP-RKF (45), KINLSQ (46), FLUSIM (47), SCIENTIST (SciTech Intl.), and PROPHET [BBN Software Products Inc., see for example (48)]. Most of these programs are not generally applicable to an arbitrary kinetic mechanism, represented symbolically by chemical equations, or are not readily available in the public domain. Therefore the merits of DYNAFIT are discussed below by way of comparison with KINSIM/FITSIM, further abbreviated as the KF method.

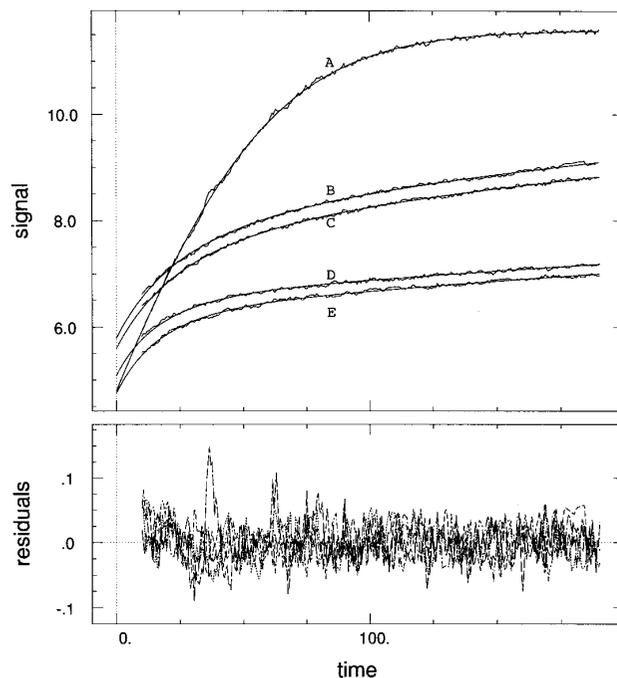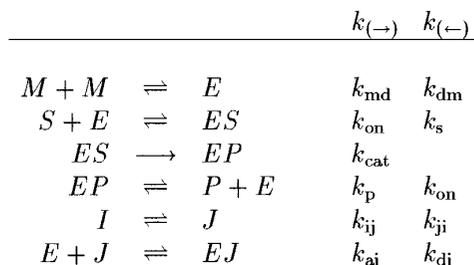Of the four example problems described above, only

FIG. 3. Global least-squares fit of progress curves collected during transient inhibition of the proteinase from HIV (nominal concentration 0.030 μM). The enzyme was the last added component in the assay. Inhibitor concentrations were held fixed at their nominal values: 0 μM (A), 0.040 μM (B, C), and 0.060 μM (D, E), as was the substrate concentration (10 μM). The nominal concentration of the enzyme (0.030 μM) in each assay was optimized within $\pm 10\%$ titration error. Fluorescence at Time 0 was also optimized for each assay. For details see text; the numerical results are summarized in Table 3.

Example 1 could be solved by the KF method at least in principle. In practice, however, FITSIM failed due to the inability to take into account titration errors. Figure 5 shows that a match between the experimental data (the jagged curves) and the theoretical model (the smooth curves) was not achieved. Under such circumstances the examination of the fitting parameters is meaningless. Nevertheless, the KF method suggests that the irreversible inhibitor has an initial binding constant of 0.0001 ± 0.3 nM and a deactivation rate constant of 50 ± 63000 s^{-1}. The uncertainties of fitting

			$k_{(\rightarrow)}$	$k_{(\leftarrow)}$
$M + M$	$\rightleftharpoons$	E	k_{md}	k_{dm}
$S + E$	$\rightleftharpoons$	ES	k_{on}	k_s
ES	$\longrightarrow$	EP	k_{cat}	
EP	$\rightleftharpoons$	$P + E$	k_p	k_{on}
I	$\rightleftharpoons$	J	k_{ij}	k_{ji}
$E + J$	$\rightleftharpoons$	EJ	k_{ai}	k_{di}

SCHEME 3

TABLE 3
Results of the Least-Squares Fit of Progress Curves Shown
in Fig. 3 to the Kinetic Model Shown in Scheme 3

Dataset (trace)	Parameter	Initial value	Fitted value
	k_{md} (μM^{-1} s^{-1})	0.1	—
	k_{dm} (s^{-1})	0.001	—
	k_{on} (μM^{-1} s^{-1})	100	—
	k_s (s^{-1})	300	374.8 ± 3.5
	k_{cat} (s^{-1})	10	7.19 ± 0.11
	k_p (s^{-1})	500	1294.3 ± 7.9
	k_{ji} (s^{-1})	1000	—
	k_{ij} (s^{-1})	20	42.06 ± 0.77
	k_i (s^{-1})	0.001	0.00197 ± 0.00004
	ϵ_P	0.7	0.682 ± 0.001
	$[S]_0$ (μM)	10	—
A	$[E]_0$ (μM)	0.030	0.0336 ± 0.0006
B		0.030	0.0270 ± 0.0005
C		0.030	0.0265 ± 0.0005
D		0.030	0.0264 ± 0.0007
E		0.030	0.0281 ± 0.0007
A	Offset	—[a]	4.794 ± 0.010
B		—[a]	5.796 ± 0.010
C		—[a]	5.600 ± 0.011
D		—[a]	5.091 ± 0.013
E		—[a]	4.751 ± 0.013

Note. The concentrations of the inhibitor were 0, 40, 40, 60, and 60 nM for traces A–E, respectively.

[a] The initial estimate of the offset was made automatically, by using the first datapoint on each progress curve.

FIG. 4. Least-squares fit of initial velocities for HIV proteinase inhibition by a substrate analog. The concentrations of the substrate were 20 μM (circles), 40 μM (squares), 80 μM (triangles up), and 120 μM (triangles down). The nominal enzyme concentration was 8 nM; the optimized value was 5.9 ± 0.4 nM. For details see text; the numerical results are summarized in Table 4.

parameters are merely the formal standard errors (14, 15) and not true confidence intervals, but even so the errors are unreasonably large for the analysis to be acceptable. The best-fit values of rate constants k_i and k_{de} (Table 1) determined by DYNAFIT or FITSIM differ by factors of 8300 and 410, respectively. The KF method hugely overestimated the potency of the inhibitor, both in terms of the binding constant and in terms of the deactivation rate constant.

Both in using DYNAFIT and in using FITSIM, the same rate constants were considered as globally optimized fitting parameters. The main difference is that in DYNAFIT we do not rigidly insist on the nominal values of concentrations. Instead, recognizing that biochemists make titration errors, each curve in Fig. 1 was assigned certain locally adjustable fitting parameters, namely the concentrations of the enzyme and the substrate in each assay. This flexibility, introduced by treating concentrations as partially unknown within 10% titration error, allowed DYNAFIT to match the data and the model reasonably well and come up with acceptably small uncertainties of inhibition constants (Table 3).

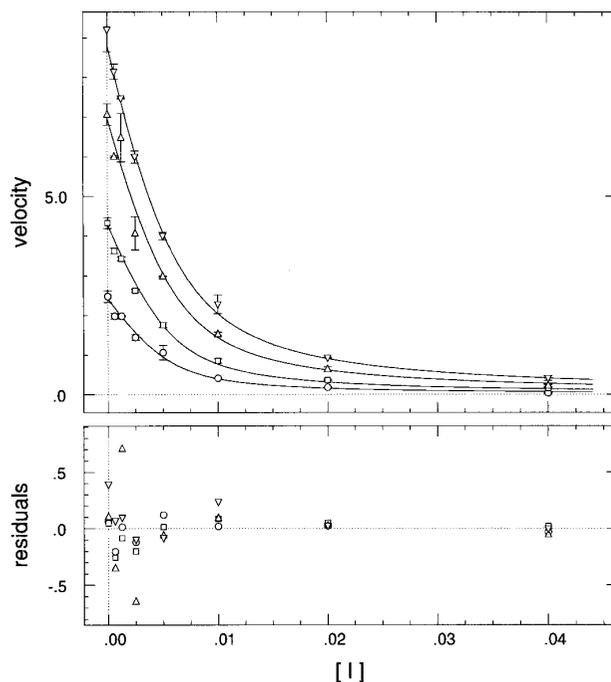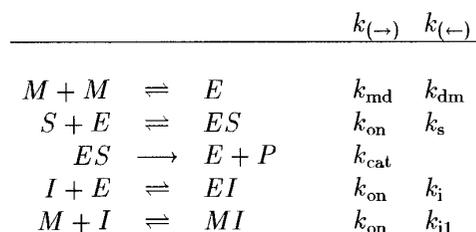The treatment of certain concentrations as partially unknown stems from theory as well as from practical experience. The theory of fitting kinetic data to sets of differential equations, and an example from industrial chemical kinetics, is presented in a classic monograph on nonlinear regression (49). Published examples of biochemical data also show that when titration errors are neglected, the global analysis of multiple progress curves cannot be successful (46). When the published data (46) were reanalyzed by using DYNAFIT, the match between the data and the model improved owing to the adjustable concentrations. The same is true for other published reports in which FITSIM was used [see for example the lower three progress curves in Fig. 1 of Ref. (38)].

The necessity of allowing for titration errors is made intuitively obvious by a thorough examination of Fig. 1. In the irreversible inhibition assays represented by

			$k_{(\rightarrow)}$	$k_{(\leftarrow)}$
$M + M$	$\rightleftharpoons$	E	k_{md}	k_{dm}
$S + E$	$\rightleftharpoons$	ES	k_{on}	k_s
ES	$\longrightarrow$	$E + P$	k_{cat}	
$I + E$	$\rightleftharpoons$	EI	k_{on}	k_i
$M + I$	$\rightleftharpoons$	MI	k_{on}	k_{i1}

SCHEME 4

TABLE 4

Results of the Least-Squares Fit of Initial Velocities Shown in Fig. 4 to the Kinetic Model Shown in Scheme 4

Round of analysis	Parameter	Initial value	Fitted value
I	k_{md} (μM^{-1} s^{-1})	0.1	—
	k_{dm} (s^{-1})	0.001	0.00009 ± 0.00299
	k_{on} (μM^{-1} s^{-1})	100	—
	k_s (s^{-1})	20000	12050 ± 26530
	k_{cat} (s^{-1})	4	3.33 ± 0.83
	k_i (s^{-1})	0.1	0.08 ± 0.23
	k_{i1} (s^{-1})	1	$10^6 \pm 4.9 \times 10^{12}$
	$[E]_0$ (μM)	0.005	0.0060 ± 0.0072
II	k_{md}	0.1	—
	k_{dm}	0.001	0.00004 ± 0.00195
	k_{on}	100	—
	k_s	20000	$12,440 \pm 24,630$
	k_{cat}	4	3.38 ± 0.58
	k_i	0.1	0.08 ± 0.23
	k_{i1}	1000000	—
	$[E]_0$	0.005	0.0059 ± 0.0070
III	k_{md}	0.1	—
	k_{dm}	0.0005	—
	k_{on}	100	—
	k_s	20000	$12,380 \pm 410$
	k_{cat}	4	3.37 ± 0.24
	k_i	0.1	0.080 ± 0.005
	k_{i1}	1000000	—
	$[E]_0$	0.005	0.0059 ± 0.0004

traces A and B, the substrate was completely consumed. This is manifested by the fact that the catalytic reaction came to a complete halt at the end of both assays. Because the substrate concentrations were the same nominally, the total fluorescence changes in these two experiments should be the same also. Note however that the total change of fluorescence was about 5% lower for trace B, in comparison with trace A. This can be explained if the experimenter delivered 5% less substrate into the assay B compared with assay A. Such a 5% titration error is comparatively large but not unusual.

Another striking illustration is provided by traces D and E. Supposedly these two assays are exact replicates, where both the enzyme and the inhibitor were nominal at 0.004 μM, but the shape of trace D is clearly different from that of trace E. The fitting parameters in Table 1 show that this difference is explained by a mere 2% difference in concentrations. In the case of trace D, the enzyme concentration was about 2% higher than the inhibitor concentration, leaving a nonnegligible amount of the catalyst after all inhibitor was irreversibly bound. That is why the reaction did not completely stop, and trace D continues to rise, showing ongoing catalysis by the protease. In the case of trace E, the amount of the inhibitor truly matched (point of equivalence) or even exceeded the enzyme, so that

when all the inhibitor was bound, the reaction could not proceed further and the progress curve became flat.

It is important to note that we made an arbitrary choice of which reactant is treated as being affected by titration errors (the enzyme) and which reactant is treated as if its concentration was known exactly (the inhibitor). In this particular test example, treating both concentrations as unknown would lead to an increase in the standard errors of fitting parameters. The important fact is that titration errors must be admitted for at least one of the reactants.

As for the test Example 2 above, a comparison with KINSIM/FITSIM is not possible, because these programs are incapable of analyzing concentration jump experiments for the following reason. FITSIM requires that the investigator provide the initial concentration of each chemical species at the beginning of the assay. In the test Example 2, however, the initial composition of the monomer/dimer mixture is not known. Only the total concentration of the enzyme is known, at least within a certain titration error, but we do not know how the total enzyme is distributed between the monomeric and dimeric forms. This distribution depends on the values of association and dissociation rate constants, which are not known in advance. In fact, the very purpose of the experiment is to determine them.
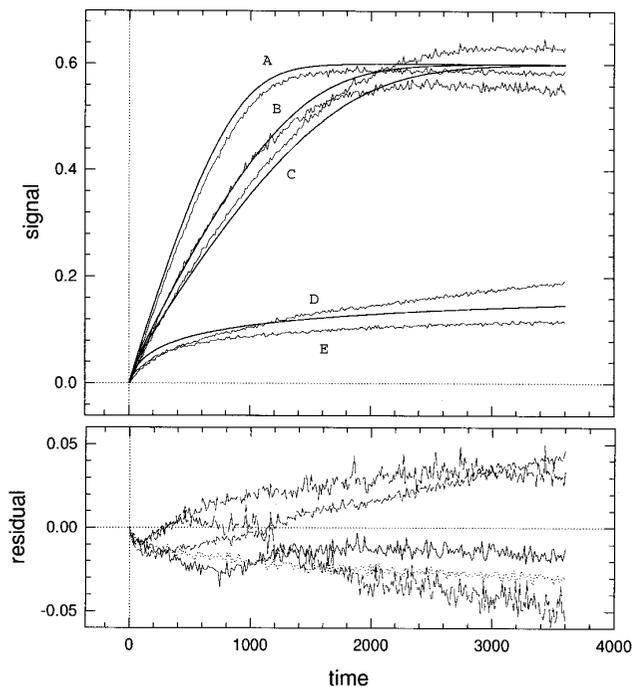

FIG. 5. Global least-squares fit by using FITSIM of progress curves collected during irreversible inhibition of the proteinase from HIV (nominal concentration 0.004 μM). The enzyme was the last added component in the assay. All concentrations were held fixed at their nominal values. For details see text; the numerical results are summarized in Table 1.

DYNAFIT approaches the problem as follows. The investigator provides an initial estimate of the association and dissociation rate constant and the total concentration of each reactant. In each step of the least-squares fit, equilibrium constants are calculated as ratios of rate constants (e.g., the dissociation rate constant $K_D = k_{off}/k_{on}$). Then the composition of the pre-equilibrated mixture is computed from the equilibrium constants, by solving a system of simultaneous algebraic equations (8). The resulting equilibrium composition is taken as the starting composition for the dynamic phase of the assay, after first reducing all equilibrium concentrations by the appropriate dilution factor. This is the concentration jump, in which stock solutions of reactants are mixed, and thus all concentrations are instantaneously decreased due to dilution. The time course of the ensuing reaction is computed as in the usual manner, by solving a system of differential equations. In the course of the iterative least-squares regression, the simulated progress curves are compared with the experimental data, and a better estimate is made of the association and dissociation rate constants. Importantly, new values of rate constants lead to new values of the equilibrium dissociation constants, which implies that a new initial composition of the preequilibrated mixture must be computed. Thus, DYNAFIT shuttles between solving multiple simultaneous equilibria, as systems of algebraic equations, and solving the reaction time course, as systems of differential equations, arriving each time at a different estimate of the starting composition.

In the case of the test Example 3, a comparison with the KF method is not possible either, because that method cannot analyze preexisting isomerization equilibria for a similar reason as in Example 2. In particular, the KF method requires that the exact composition at the beginning of the assay be known beforehand. Consequently, it cannot treat isomerization rate constants as adjustable parameters. As for test Example 4, the KF method cannot be used, because it has no capability of analyzing initial velocities.

PROGRAM DESCRIPTION

This section describes the basic technical parameters of DYNAFIT, the required computer hardware and operating systems, the kinds of input data that are used, and the types of output generated.

DYNAFIT can simulate or fit up to 16 progress curves in a global dataset, which can contain a total of 16,000 datapoints. An unlimited number of individual progress curves, each of them containing up to 1500 datapoints, can be simulated or fitted in one run. Initial velocity data may contain up to 1024 datapoints, with one or two simultaneously varied concentrations. The reaction mechanism may contain up to 64 chemical species participating in 128 individual reaction steps. The molecularity of the reaction steps in the mechanism may be in the range from zero to four. The data simulation module utilizes the normal or Gaussian distribution of experimental noise. The present version of DYNAFIT cannot handle biochemical reactions during which the pH, ionic strength, temperature, or pressure changes over time.

The program consists of 33,558 lines of source code written in the ANSI Fortran-77 language. It can be used on hardware platforms ranging from desktop personal computers (both the IBM-PCs and the Macintosh models) to workstations (S.G.I., IBM RISC/System 6000, DEC Alpha) to mainframes (VAX) to supercomputers (Cray Y/MP and C90). For an efficient execution of DYNAFIT, desktop personal computers are required to have installed at least eight million bytes of random-access memory and special hardware for floating-point arithmetic (math coprocessor). A typical example is a desktop IBM-PC-compatible machine equipped with the Intel i486 or Pentium processor or a Macintosh computer with the Motorola MC68040 or PowerPC 604 processor. The performance of different computers running DYNAFIT is shown in Table 5.

As can be seen from Table 5, the truncation and round-off errors caused the least-squares fit to take different numbers of iterations not only on different machines, but also on the same computer but using two different compilers. This subtle machine dependence is a manifestation of the very large number of elementary arithmetic operations that are involved in each fit. The differences are caused mostly by the different designs of the special hardware and the low-level software for floating-point arithmetic. The most precise results were obtained on the Cray supercomputer, because that machine can represent floating-point numbers by the largest number of bits. Personal computers without the special math coprocessor, including some PowerPC Macintosh models, or computers with low-grade central processing units such as Intel 80386 or Motorola 68030 are unsuitable for running DYNAFIT. Not only do the computation times increase beyond practical limits, for example, the test Example 1 took 18 h of continuous computation on a Macintosh SE30, but also the severe loss of precision on low-grade machines causes the computation to run in circles.

The input for DYNAFIT are ASCII text files and a system of interactive on-screen menus. The program utilizes three different types of input for each run. The first type of ASCII input files are the experimental data. Both the progress curves and the initial velocity data are arranged in columns (e.g., time and absorbance or concentration and velocity). The program can analyze progress curves from uniresponse or multiresponse observations (e.g., simultaneous spectrophotometry at different wavelengths). The

TABLE 5

Performance of Different Computers Running the Program DYNAFIT

Computer	Example 1	Example 2	Example 3	Example 4	Parameter[a]
i486[b]	25/43/78	25/51/87	38/28/85	8/0/9	n
	10.76	1.274	8.724	0.3242	t
	1.56133	0.388029	1.78933	21.3586	χ^2
i486[c]	24/31/66	25/51/87	100[d]/44/191	8/0/9	n
	7.32	1.105	16.88	0.4440	t
	1.55028	0.388109	1.74924	21.3586	χ^2
Pentium[e]	20/30/61	25/51/87	100[d]/45/194	13/22/44	n
	2.421	0.4222	6.420	0.2702	t
	1.55114	0.398450	1.74926	21.8413	χ^2
Mac Quadra[f]	26/51/92	37/68/120	100[d]/45/195	13/22/44	n
	24.79	4.322	50.06	1.728	t
	1.53865	0.387459	1.76265	21.8413	χ^2
Power Mac[g]	49/78/159	25/49/84	100[d]/46/193	13/22/44	n
	14.33	0.9942	15.44	0.7022	t
	1.55255	0.388300	1.75217	21.8413	χ^2
SGI Iris[h]	37/35/93	25/51/87	75/48/162	13/22/44	n
	2.524	0.2760	2.971	0.2212	t
	1.54560	0.388095	1.76902	21.8413	χ^2
DEC Alpha[i]	33/36/89	25/51/86	100[d]/46/191	13/22/44	n
	1.863	0.2155	3.538	0.1112	t
	1.54518	0.388288	1.75445	21.8413	χ^2
IBM RISC[j]	18/31/59	25/51/86	100[d]/46/191	8/0/9	n
	1.476	0.2581	4.230	0.1437	t
	1.53877	0.388097	1.75721	21.3586	χ^2
Cray single[k]	88/105/247				n
	4.774	—	—	—	t
	1.58396				χ^2
Cray double[l]	19/42/83	25/51/86	100[d]/45/93	8/0/9	n
	2.326	0.2813	4.523	0.1728	t
	1.53932	0.388052	1.75001	21.3586	χ^2

[a] n, number of iterations/subiterations/function evaluations in the Levenberg–Marquardt–Reich least-squares fitting algorithm; t, wall-clock execution time in minutes; χ^2, final reduced χ^2.

[b] A generic PC-compatible computer equipped with an Intel 80486/DX2 processor running at 66 MHz under the DOS 6.22 and Windows 3.1 operating system. Compiled with Microsoft 32-bit Fortran PowerStation ver. 1 (compiler flags: /G4/Ox/Op/D "NDEBUG").

[c] Compiled with Watcom Fortran-77 ver. 10.5 (compiler flags: -sa-al-ot).

[d] Regression was terminated due to the lack of convergence.

[e] International Bussines Machines Corp., Model PC-750, Intel-Pentium processor running at 90 MHz under the Windows 95 operating system. Compiled with Watcom Fortran-77 ver. 10.5 (compiler flags: -sa-al-ot).

[f] Apple Computer, Model Quadra 840av, Motorola 68040 processor plus 68881 math coprocessor running at 25 MHz under MacOS 7.1. Compiled with Language Systems Fortran ver. 3.3 (compiler flags: -bkg = 2 -opt = 1 -mc68040-FPU -saveall).

[g] Apple Computer, Model Power Macintosh 8500, IBM–Motorola PowerPC 604 processor plus math coprocessor running at 120 MHz under MacOS 7.5. Compiled with Language Systems Fortran for Power Macintosh ver. 1.0 (compiler flags: -bkg = 2 -opt = 1 -saveall).

[h] Silicon Graphics Inc., Model Iris Indigo, MIPS-4000 processor running at 100 MHz under the IRIX 5.3 Unix operating system. Compiled with the SGI f77-compiler (flags: -mips2 -static -O).

[i] Digital Equipment Corp., Alpha processor running at 150 MHz under the DEC OSF/1 2.1B Unix operating system. Compiled with the DEC f77-compiler (flags: -O2).

[j] International Bussines Machines Corp., RISC System/6000 Type 7013 Model 580, IBM–Motorola PowerPC 604 processor running at 120 MHz under the AIX 3.2 Unix operating system. Compiled with the xlf-compiler (flags: -O).

[k] Cray Computers, Model C90 eight-processor supercomputer running under the UNICOS 8.0.4 operating system. Compiled with the Cray Research, Inc. cf77-compiling system (flags: -Wf"-dp -a static" -Zv). Floating point numbers represented in the Cray single-precision 64-bit format.

[l] As above, with compiler flags: -Wf"-a static" -Zv. Floating point numbers represented in the Cray double-precision 128-bit format.

```
; DYNAFIT script file ./test/hiv-prot/comptit/mondim.par
; -------------------------------------------------------
; Tight inhibitor binds to monomer and dimer. Example 4.

[mechanism]
   M + M <==> E     :     kmd    kdm
   E + S <==> ES    :     kon    kds
   ES ---> E + P    :     kr
   E + I <==> EI    :     kon    ki
   M + I <==> MI    :     kon    ki1

[rate constants]
   kmd = 0.1, kdm = 0.0001 ?, ki = 0.1 ?, ki1 = 1 ?
   kon = 100, kds =  14000 ?, kr = 4 ?

[responses]
   P = 1000

[concentrations]
   E = 0.005 ?

[velocity]
   file            ./test/hiv-prot/comptitr/dat/e10is.tab
   columns         I, S
   equilibrate     E + S + I, dilute 1:1

[data]
   error           constant 0.01
   delay           -1 ; rapid equilibrium approximation

[end]
```

FIG. 6.   DYNAFIT input data for Example 4. Additional input consists of a four-column ASCII text file, as indicated in the "[velocity]" section. The first two columns contain the concentrations of the inhibitor and the substrate, the third column holds the initial velocity, and the fourth column contains the standard error of each measurement computed from replicates.

readings of time can be nonevenly spaced, and different progress curves in a global dataset might contain different numbers of datapoints. Such technical details are important for the practical usefulness of a data analysis program. For example, FITSIM can be used only with progress curves that contain the same number of equally spaced datapoints. To satisfy this requirement, some users of FITSIM made up artificial datapoints by interpolation (44).

The second type of input are text files which store miscellaneous control parameters, approximately 100 in total, such as how many iterations are to be performed in the nonlinear least-squares fit and what are the desired convergence tolerances. Each problem can be assigned different sets of control parameters.

The third type of input data are script files which describe the reaction mechanism and the initial estimates of fitting parameters and identify the location of data files in the computer's file system. File names are freely interchangeable between the DOS/Windows, Macintosh, and Unix file naming conventions. Thus, for example, ".\TEST\FILE.TXT" (DOS and Windows), "::TEST:FILE.TXT" (Macintosh), and "./TEST/FILE.TXT" (Unix) can substitute for one another. This allows portability of data files from one type of computer to another. Figures 6 and 7 show examples of

input script files for fitting initial velocities (test Example 4) and for fitting progress curves (test Example 1), respectively. The order of sections, denoted by square brackets in the script file, is entirely arbitrary. Only a few rules apply to the arrangement of items within each section. DYNAFIT thus utilizes a rudimentary scripting language with loose syntax and a small vocabulary consisting of keywords such as "file," "column" (in a text file), "concentration," "equilibrate," "error," "linear," or "delay."

On personal computers (IBM-PC and Macintosh), DYNAFIT generates high-resolution on-screen color graphics. On the Unix workstations and mainframes, DYNAFIT produces rudimentary graphical patterns composed of letters, numerals, and other symbols in the ASCII character set.

The results of fit are written on the disk as tab-delimited ASCII text files, so that many computer programs for scientific graphics can be used to produce publication-quality illustrations. In addition, all graphical images produced by DYNAFIT are written on disk as encapsulated PostScript files (50) suitable for viewing or printing on PostScript devices. For example, Figs. 1 through 4 were automatically generated by DYNAFIT in the PostScript format.

```
; DYNAFIT script file ./test/hiv-prot/irrevers/irrev.par
; -------------------------------------------------------
; Irreversible inhibition of HIV proteinase. Example 1.

[mechanism]
   M + M <==> E     :  ka    kd
   E + S <==> ES    :  kon   ks
   ES ---> E + P    :  kr
   E + P <==> EP    :  kon   kp
   E + I <==> EI    :  kon   ki
   EI --> EJ        :  kde

[rate constants]
   ka = 0.1, kd = 0.0001, ki = 0.1 ?, kde = 0.1 ?
   kon = 100, ks = 300 ?, kr = 10 ?, kp = 500 ?

[responses]
   P = 0.024 ?

[concentrations]
   local E = 0.004 ?, S = 25 ?

[data]
   directory   ./test/hiv-prot/irrevers/dat/
   extension   txt
   error       constant 0.003
   offset      auto ?
   delay       0
   mesh        from 0 to 3800 step 10
   file        2o, 3o, 5o, 7o, 8o
   vary conc. I =  0, 0.003, 0.0015, 0.004, 0.004

[settings]
   ./test/hiv-prot/irrevers/hivnci.def

[end]
```

FIG. 7.   DYNAFIT input data for Example 1. Additional input consists of two-column ASCII progress curve files, as indicated in the "[data]" section.
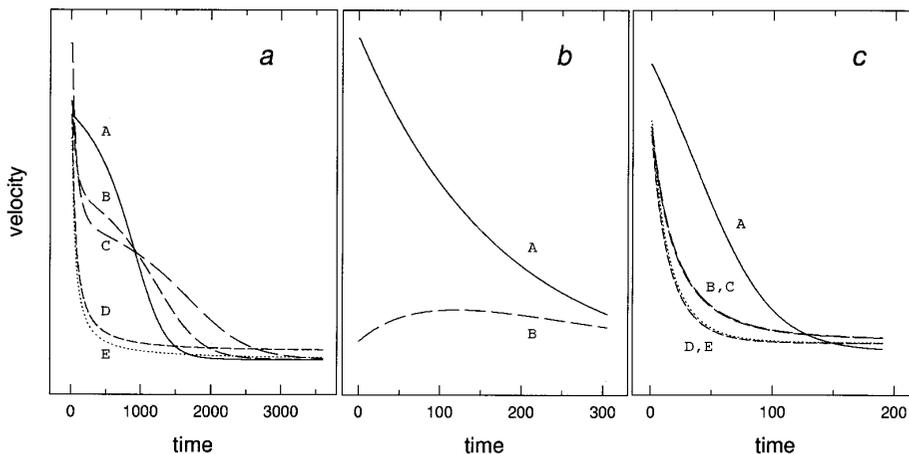
FIG. 8. Evolution in time of the reaction velocities or derivatives of progress curves. (a) Curves A–E are first derivatives of curves A–E in Fig. 1. Note that curves B and C show more clearly the biphasic reaction. In the first phase the rate decreases rapidly due to the covalent binding of the irreversible inhibitor. In the second phase the rate decreases less rapidly due to substrate depletion. Also note that the residual velocity is greater than zero for curve D, because 2% less inhibitor than the enzyme was present in the assay. (b) Curves A and B are first derivatives of curves A and B in Fig. 2. The lag phase, or inflection point, on the convex progress curve B in Fig. 2 is manifested more clearly, as a maximum on the derivative curve B. (c) Curves A–E are first derivatives of curves A–E in Fig. 3. See comments in the text.

Program DYNAFIT generates optionally the first derivative plots of progress curves (Fig. 8). Such derivative plots, produced also by the program FLUSIM (47), are useful in detecting subtle features in the original progress curves. For example, Fig. 8b shows how the slopes of progress curves in Fig. 2 change over time. This derivative plot clearly shows that trace B in Fig. 2 initially speeds up, due to the substrate-induced assembly of the HIV proteinase dimer (30), and then slows down, due to substrate depletion and enzyme denaturation. The derivative plot in Fig. 8a shows that the slope of trace A in Fig. 1 is decreasing markedly immediately from the very beginning of the assay. This contradicts the intuition. Many enzymologists would probably claim that the initial part of the progress curve A in Fig. 1 is linear (a region of constant velocity), but the derivative trace A in Fig. 8a shows that this is not so. The derivative or velocity is changing rapidly from the start. This is even more pronounced in trace A of Fig. 8c, which corresponds to trace A in Fig. 3. Also note that the traditional analysis of transient or slow-binding inhibition requires that progress curve B in Fig. 3 contain a region of constant or steady-state velocity. However, the derivative trace B in Fig. 8c shows that in actuality the velocity keeps decreasing due to substrate depletion.

DYNAFIT generates LaTeX files for direct typesetting (51, 52). After the reaction mechanism is translated from the symbolic form, the underlying mathematical equations are derived and typeset. For example, as the input script in Fig. 7 is processed, DYNAFIT typesets not only Scheme 1 but also the corresponding Eqs. [1] through [9].

$$d[M]/dt = -2k_{md}[M][M] + 2k_{dm}[E] \qquad [1]$$

$$d[P]/dt = k_r[ES] - k_{on}[P][E] + k_p[EP] \qquad [2]$$

$$d[S]/dt = -k_{on}[S][E] + k_s[ES] \qquad [3]$$

$$d[I]/dt = -k_{on}[I][E] + k_i[EI] \qquad [4]$$

$$d[ES]/dt = k_{on}[S][E] - k_s[ES] - k_r[ES] \qquad [5]$$

$$d[EP]/dt = k_{on}[P][E] - k_p[EP] \qquad [6]$$

$$d[E]/dt = k_a[M][M] - k_d[E] - k_{on}[S][E]$$
$$+ k_s[ES] + k_r[ES] - k_{on}[P][E] + k_p[EP]$$
$$- k_{on}[I][E] + k_i[EI] \qquad [7]$$

$$d[EI]/dt = k_{on}[I][E] - k_i[EI] - k_{de}[EI] \qquad [8]$$

$$d[EJ]/dt = k_{de}[EI] \qquad [9]$$

In summary, program DYNAFIT is a new computational tool for biochemical kinetics which extends the capabilities of the KF method (1, 2) in at least four ways. First, DYNAFIT can analyze initial velocity data. Second, it can treat concentrations as adjustable fitting parameters. This is necessary not only to achieve a close fit of multiple progress curves, but also it can be used for active-site titrations. Third, the program can analyze progress curves from concentration jump experiments and progress curves that reflect preexisting isomerization equilibria. Finally, DYNAFIT can treat as adjustable parameters certain instrumental properties, such as molar response coefficients (e.g., the specific molar absorbtivity) or background instrumental signal (e.g., the baseline absorbance). Recently we uti-

lized these features in determining the mechanism of inhibition for human 5α-keto-steroid reductase II (53). The program is available free of charge to all interested parties, upon sending a blank formatted disk in a self-addressed stamped envelope to the author. It is also available via the Internet by anonymous ftp from uwm ml.pharmacy.wisc.edu (directory ./pub/dynafit) or on the World Wide Web page http://uwmml.pharmacy.wi sc.edu.

REFERENCES

1. Barshop, B. A., Wrenn, R. W., and Frieden, C. (1983) *Anal. Biochem.* 130, 134–145.
2. Zimmerle, C. T., and Frieden, C. (1989) *Biochem. J.* 258, 381–387.
3. Cleland, W. W. (1967) *Adv. Enzymol. Rel. Areas Mol. Biol.* 29, 1–32.
4. Segel, I. H. (1975) Enzyme Kinetics—Behavior and Analysis of Rapid Equilibrium and Steady-State Enzyme Systems, Wiley, New York.
5. Kuby, S. A. (1991) A Study of Enzymes, CRC Press, Boca Raton, FL.
6. Garfinkel, D., Ching, S. W., Adelman, M., and Clark, P. (1966) *Ann. N.Y. Acad. Sci.* 128, 1054–1068.
7. Hayashi, K., and Sakamoto, N. (1985) Dynamic Analysis of Enzyme Systems—An Introduction, Springer-Verlag, New York.
8. I, T.-P., and Nancollas, G. H. (1972) *Anal. Chem.* 44, 1940–1950.
9. Hindmarsh, A. C. (1983) *in* Scientific Computing (Stepleman, R. S., *et al.,* Eds.), pp. 55–64, North-Holland, Amsterdam.
10. Petzold, L. R. (1983) *in* Scientific Computing (Stepleman, R. S., *et al.,* Eds.), pp. 65–74, North-Holland, Amsterdam.
11. Reich, J. G. (1992) Curve Fitting and Modelling for Scientists and Engineers, McGraw-Hill, New York.
12. Seber, G. A. F., and Wild, C. J. (1989) Nonlinear Regression, Wiley, New York.
13. Mannervik, B. (1982) *Methods Enzymol.* 87, 370–390.
14. Press, W. H., Teukolsky, S. A., Vetterling, W. T., and Flannery, B. P. (1992) Numerical Recipes in C, Cambridge Univ. Press, Cambridge.
15. Bevington, P. R. (1969) Data Reduction and Error Analysis in Physical Sciences, McGraw-Hill, New York.
16. Rawlings, J. O. (1988) Applied Regression Analysis—A Research Tool, Wadsworth, Belmont.
17. Rayner, J. C. W., and Best, D. J. (1989) Smooth Tests of Goodness of Fit, Oxford Univ. Press, New York.
18. Draper, N., and Smith, H. (1981) Applied Regression Analysis, Wiley, New York.
19. Mannervik, B. (1981) *in* Kinetic Data Analysis—Design and Analysis of Enzyme and Pharmacokinetic Experiments (Endrenyi, L., Ed.), pp. 235–270, Academic Press, New York.
20. D'Agostino, R. B. (1986) *in* Goodness-of-Fit Techniques (D'Agostino, R. B., and Stephens, M. A., Eds.), pp. 7–62, Dekker, New York.
21. Hamaker, H. C. (1978) *Appl. Stat.* 27, 76–79.
22. Belsley, D. A., Kuh, E., and Welsch, R. E. (1980) Regression Diagnostics—Identifying Influential Data and Sources of Variation, Wiley, New York.
23. Smith, W. R., and Missen, R. W. (1982) Chemical Reaction Equilibrium Analysis, Wiley, New York.
24. Royer, C. A., and Beechem, J. M. (1992) *Methods Enzymol.* 210, 481–505.
25. Alberty, R. A. (1994) *Biophys. Chem.* 49, 251–261.
26. Bjornbom, P. (1981) *Ind. Eng. Chem. Fundam.* 20, 161–164.
27. Martell, A. E., and Motekaitis, R. J. (1988) Determination and Use of Stability Constants, VCH Publ., New York.
28. Peranteau, A. G., Kuzmič, P., Angell, Y., García-Echeverría, C., and Rich, D. H. (1995) *Anal. Biochem.* 227, 242–245.
29. Beechem, J. M. (1992) *Methods Enzymol.* 210, 37–54.
30. Kuzmič, P., García-Echeverría, C., and Rich, D. H. (1993) *Biochem. Biophys. Res. Commun.* 194, 301–305.
31. Pargellis, C. A., Morelock, M. M., Graham, E. T., Kinkade, P., Pav, S., Lubbe, K., Lamarre, D., and Anderson, P. C. (1994) *Biochemistry* 33, 12527–12534.
32. Giroux, E. (1991) *J. Enzyme Inhib.* 5, 249–257.
33. Toth, M. V., and Marhall, G. R. (1991) *Int. J. Pept. Protein Res.* 36, 544–550.
34. Frieden, C. (1990) *Proc. Natl. Acad. Sci. USA* 87, 4413–4416.
35. Kurz, L. C., Moix, L., Riley, M. C., and Frieden, C. (1992) *Biochemistry* 31, 39–48.
36. Rodriguez, E. J., Debouck, C., Deckman, I. C., Abusoud, H., Raushel, F. M., and Meek, T. D. (1993) *Biochemistry* 32, 3557–3563.
37. Kati, W. M., Johnson, K. A., Jerva, L. F., and Anderson, K. S. (1992) *J. Biol. Chem.* 267, 5988–5997.
38. Francisco, W. A., Abusoud, H. M., Baldwin, T. O., and Raushel, F. M. (1993) *J. Biol. Chem.* 268, 24734–24741.
39. Lembert, N., and Idahl, L. A. (1995) *Biochem. J.* 305, 929–933.
40. Shearer, G. L., Kim, K. Y., Lee, K. M., Wang, C. K., and Plapp, B. V. (1993) *Biochemistry* 32, 11186–11194.
41. Sheehan, J. P., Wu, Q. Y., Tollefsen, D. M., and Sadler, J. E. (1993) *J. Biol. Chem.* 268, 3639–3645.
42. Gassner, G., Wang, L. H., Batie, C., and Ballou, D. P. (1994) *Biochemistry* 33, 12184–12193.

43. Moore, K. J. M., and Lohman, T. M. (1994) *Biochemistry* 33, 14565–14578.

44. Ali, J. A., Orphanides, G., and Maxwell, A. (1995) *Biochemistry* 34, 9801–9808.

45. Duggleby, R. G. (1994) *Biochim. Biophys. Acta* 1205, 268–274.

46. Gutheil, W. G., Kettner, C. A., and Bachovchin, W. W. (1994) *Anal. Biochem.* 223, 13–20.

47. Machleidt, W., Nagler, D. K., Assfalg-Machleidt, I., Stubbs, M. T., Fritz, H., and Auerswald, E. A. (1995) *FEBS Lett.* 361, 185–190.

48. Groebe, D. R., and Abramson, S. N. (1995) *J. Biol. Chem.* 270, 281–286.

49. Bard, Y. (1974) Nonlinear Parameter Estimation, Academic Press, New York.

50. McGilton, H., and Campione, M. (1992) PostScript by Example, Addison-Wesley, Reading.

51. Ramport, L. (1986) LaTeX—A Document Preparation System, Addison-Wesley, Reading.

52. Buerger, D. J. (1990) LaTeX for Engineers and Scientists, McGraw-Hill, New York.

53. Moss, M. L., Kuzmič, P., Stuart, J. D., Tian, G., Peranteau, A. G., Frye, S. V., Kadwell, S. H., Kost, T. A., Overton, L. K., and Patel, I. R. (1996) *Biochemistry* 35, 3457–3464.